An Accurate 1D Camera Calibration Based on Weighted Similar-Invariant Linear Algorithm

Lixia Lin[1], Lijun Wu[1](✉), Songlin Lai[1], Zhicong Chen[1], Peijie Lin[1], and Zhenhui Wu[2]

[1] College of Physics and Information Engineering, Fuzhou University, Fuzhou 350116, China
lijun.wu@fzu.edu.cn

[2] State Grid Fuzhou Electric Power Supply Company, Fuzhou 350116, China

Abstract. In recent years, researchers around the world have been researching and improving the technique of 1D calibration of cameras. The previous work has been primarily focused on reducing the motion constraints of one-dimensional calibration objects, however the accuracy of the existing methods still needs to be improved when random noise is introduces. In order to improve the accuracy of the one-dimensional calibration of the camera, in this paper, we propose a new calibration method by combining a weighted similar invariant linear algorithm and an improved nonlinear optimization algorithm. Specifically, we use the weighted similar invariant linear algorithm to obtain the camera parameters as the initial calibration parameters, and then optimize the parameters by using improved nonlinear algorithm. Finally, in the case of introducing random noise, the results of computer simulations and laboratory experiments show that when the noise level reaches 2 pixels, the parameter error of this method is mostly reduced to 0.2% compared with other methods, which verifies the feasibility of our proposed method.

Keywords: Camera calibration · Linear algorithm · Nonlinear optimization · 1D calibration objects

1 Introduction

Camera calibration is an essential step to extract metric information from 2D images in the fields of computer vision. According to the dimension of the calibration object, the existing camera calibration techniques are roughly classified into four categories: three-dimensional reference object based calibration (3D) [1–3], two-dimensional plane based calibration (2D) [4–6], one-dimensional line based calibration (1D) [7–10] and zero-dimensional calibration (0D) [11,12]. In particular, the techniques of 1D calibration are mainly applied to calibrate the relative geometric relationships between multiple cameras and the internal parameters

R. Chamchong and K. W. Wong (Eds.): MIWAI 2019, LNAI 11909, pp. 64–75, 2019.
https://doi.org/10.1007/978-3-030-33709-4_6

of each individual camera. The techniques of 0D calibration require the multiple parameter estimations and hence involve many complicated mathematical problems. Therefore, considering the Euclidean information of collinearity and distance between the markers on the calibration object, the techniques of 1D calibration are superior to the 0D calibration in the terms of algorithm complexity, stability and accuracy. Compared to the 2D and 3D calibration methods, the 1D calibration method makes it easier to construct the calibration because the geometry required for the 1D calibration object has been reduced to a 1D object with at least three points. Moreover, the 1D calibration object does not have its own occlusion and can be simultaneously observed by all the cameras in a multi-camera system for calibration, and hence the cumbersome and cumulative errors caused by the occlusion in 2D and 3D calibration process can be avoided.

Generally, the 1D calibration algorithm includes two steps: to calculate the closed-form solution of calibration parameters and to optimize the parameter nonlinearly (see the Levenberg–Marquardt (LM) nonlinear nonlinear algorithm in [13,14]). As a typical solution of 1D calibration, Zhang's 1D calibration algorithm [7] is sensitive to the inherent noise on image point and the 1D calibration result is not precise enough. Therefore, the camera parameters initially obtained by the Zhang's 1D calibration algorithm often possess large errors. Franca et al. [15] used the Hartley's normalization algorithm to suppress noise and hence improve the 1D calibration accuracy. In fact, the elements of the 1D calibration measurement matrix are the product of the measurement data, so that each element contains different noise. However, the normalization method does not fully consider the characteristics of each measurement data, so it can only partially attenuate the effects of noise. Kunfeng et al. [16] proposed a similarity-invariant linear based 1D calibration algorithm, which does not require the normalization of image points and has higher precision than the normalized linear algorithm. Moreover, a weighted similarity-invariant linear algorithm (WSILA) is also given in their work, which can improve the calibration accuracy to certain extent. Liang et al. [17] proposed a 1D calibration method for cameras based on Heteroscedastic Error-in-Variables (HEIV) model. In their work, not only the camera parameters but also the image coordinates of the measuring points are optimized. Although the parameter error is further reduced, the computational complexity is high. The above methods have greatly improve the precision of 1D camera calibration when the noise level is low, however when the noise level is increased the calibration precision is decreased dramatically. That is because the rotation angle of the 1D calibration is regarded as a constant value during the nonlinear optimization step, which limits the calibration precision.

In this work, we propose an improved accurate 1D camera calibration based on the WSILA algorithm, which updates the rotation angle of 1D calibration object during the nonlinear optimization step. In this way, the accuracy can be greatly improved. The structure of this paper is organized as follows. The camera model and the 1D calibration object is given in Sect. 2. In Sect. 3, we introduce the principle of the 1D calibration algorithm. In Sect. 4, an improved 1D calibration algorithm is introduced, which combines weighted similar-invariant lin-

ear algorithm and an improved nonlinear optimization procedure. Experimental results of both simulation and practical experiments are given in Sect. 5. Finally, conclusions are given in Sect. 6.

2 Preliminaries

2.1 Camera Model

The coordinates of the 3D space point are expressed as $M = [X \quad Y \quad Z]^T$. The coordinates of the 2D plane point are expressed as $m = [u \quad v]^T$. The corresponding homogeneous vector are denoted as $\tilde{M} = [X \quad Y \quad Z \quad 1]^T$ and $\tilde{m} = [u \quad v \quad 1]^T$, respectively. According to the standard pinhole imaging model, the relationship between point in 3D space and its planar image point can be described as:

$$s\tilde{m} = K\,[R \quad t]\,\tilde{M} \qquad K = \begin{bmatrix} \alpha & \gamma & u_0 \\ 0 & \beta & v_0 \\ 0 & 0 & 1 \end{bmatrix} \tag{1}$$

where s is the scale factor, R and t are the rotation matrix and the translation vector, respectively, which are used to describe the relationship between the world coordinate system and the camera coordinate system. Without loss of generality, assuming that the camera coordinate system coincides with the world coordinate system, then $R = I_3$ and $t = 0_{1\times 3}$, where I_3 is 3×3 the unit matrix. K is the internal parameter matrix of the camera, with α and β are the scale factors in the image u and v axes. γ is the parameter describing the skew of the two image axes, and $[u_0 \quad v_0]$ is the coordinates of the principal point. Therefore, Eq. 1 can be expressed as:

$$s\tilde{m} = K\tilde{M} \tag{2}$$

2.2 1D Calibration Object

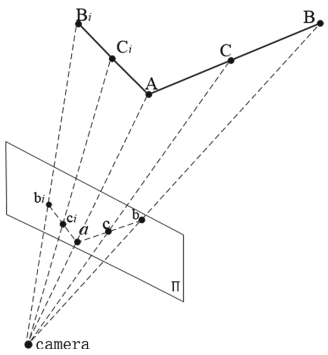

Fig. 1. Illustration of 1D calibration objects.

As shown in Fig. 1, it is assumed that the 1D calibration is composed of three points A, B and C, which satisfies $||C - A|| = L_1$, $||B - A|| = L$. The marker point A is a fixed point, the 1D calibration object rotates around it N times. A, B and C are the coordinates of the 1D calibration at the initial position, and B_i and C_i are the coordinates of points B and C when they are rotated at i-th times. The corresponding image coordinates are a_i, b_i and c_i.

3 The Principle of 1D Calibration

In this section, a variety of calibration algorithms that obtain the camera parameters from multiple observations of an 1D object are detailed.

3.1 Zhang's 1D Calibration Algorithm (ZLA)

According to Fig. 1, since the relative positions of the marker points are known, the collinearity of the three marker points A, B and C can be derived:

$$C = (1 - \lambda) A + \lambda B \tag{3}$$

where $\lambda = L_1/L$, for the convenience of calculation, $\lambda = 0.5$ is usually set. Suppose the projection points of A, B and C are a, b and c, and their Z coordinates are z_A, z_B and z_C, respectively. From Eq. 2, we have:

$$\begin{aligned} A &= z_A K^{-1} \tilde{a} \\ B &= z_B K^{-1} \tilde{b} \\ C &= z_C K^{-1} \tilde{c} \end{aligned} \tag{4}$$

Substituting the Eq. 4 into the Eq. 3, and simultaneously multiplying on both sides, there is:

$$z_B = -z_A \frac{(1 - \lambda)(\tilde{a} \times \tilde{b})(\tilde{b} \times \tilde{c})}{(\tilde{b} \times \tilde{c})(\tilde{b} \times \tilde{c})} \tag{5}$$

The Euclidean distance between endpoints A and B can be expressed as:

$$L = ||B - A|| = ||z_B K^{-1} \tilde{b} - z_A K^{-1} \tilde{a}|| \tag{6}$$

Substituting them into Eq. 5 yields:

$$z_A \left\| K^{-1} \left(\frac{(1-\lambda)(\tilde{a} \times \tilde{b})(\tilde{b} \times \tilde{c})}{(\tilde{b} \times \tilde{c})(\tilde{b} \times \tilde{c})} \right) + \tilde{a} \right\| = L \tag{7}$$

It is equivalent to:

$$\begin{aligned} z_A^2 h^T K^{-T} K^{-1} K^{-T} &= L^2 \\ h &= \tilde{a} + \frac{(1 - \lambda)(\tilde{a} \times \tilde{b})(\tilde{b} \times \tilde{c})}{(\tilde{b} \times \tilde{c})(\tilde{b} \times \tilde{c})} + \tilde{b} \end{aligned} \tag{8}$$

Let

$$\omega = K^{-T}K^{-1} = \begin{bmatrix} \omega_{11} & \omega_{12} & \omega_{13} \\ \omega_{12} & \omega_{22} & \omega_{23} \\ \omega_{13} & \omega_{23} & \omega_{33} \end{bmatrix}$$

$$= \begin{bmatrix} \frac{1}{\alpha^2} & -\frac{\gamma}{\alpha^2\beta} & \frac{v_0\gamma - u_0\beta}{\alpha^2\beta} \\ -\frac{\gamma}{\alpha^2\beta} & \frac{\gamma^2}{\alpha^2\beta^2} + \frac{1}{\beta^2} & -\frac{\gamma(v_0\gamma - u_0\beta)}{\alpha^2\beta^2} - \frac{v_0}{\beta^2} \\ \frac{v_0\gamma - u_0\beta}{\alpha^2\beta} & -\frac{\gamma(v_0\gamma - u_0\beta)}{\alpha^2\beta^2} - \frac{v_0}{\beta^2} & -\frac{(v_0\gamma - u_0\beta)^2}{\alpha^2\beta^2} + \frac{v_0^2}{\beta^2} + 1 \end{bmatrix} \tag{9}$$

The matrix is a symmetric matrix, which is defined as

$$\varpi = [\omega_{11} \quad \omega_{12} \quad \omega_{22} \quad \omega_{13} \quad \omega_{23} \quad \omega_{33}]^T \tag{10}$$

and $x = z_A^2$. Let $v = \begin{bmatrix} h_1^2 & 2h_1h_2 & h_2^2 & 2h_1h_3 & 2h_2h_3 & h_3^2 \end{bmatrix}^T$, therefore, Eq. 8 is rewritten as:

$$v^T x = L^2 \tag{11}$$

When observing N images of a 1D object, we get Eq. 12 by stacking n such Eq. 11:

$$\mathbf{V}^T x = L^2\mathbf{1} \tag{12}$$

where $\mathbf{V} = [v_1, \cdots, v_n]^T$ and $\mathbf{1} = [1, \cdots, 1]^T$. Then x can be solved according to Eq. 13:

$$x = L^2(\mathbf{V}^T\mathbf{V})^{-1}\mathbf{V}^T\mathbf{1} \tag{13}$$

According to x, the symmetric matrix can be acquired. After a simple matrix operation, the parameter K can be finally obtained to realize the camera 1D calibration.

3.2 Franca et al.'s Normalized Linear Algorithm (FNLA)

To reduce the impact of image noise on Zhang's linear algorithm, Franca et al. calibrate the camera using normalized image points. The normalization steps are operated as follows:

(1) *Translating the 2D coordinate point so that its centroid is at the origin;*
(2) *Scale the points so that their average distance to the origin is equal to* $\sqrt{2}$;
(3) *The above transformation is performed independently for each image.*

In this work, the image normalization matrix is denoted as T that is applied to transform the image point $\tilde{m}$ for obtaining the normalized image points $\hat{\tilde{m}} = T\tilde{m}$. In this way, Eq. 2 can be written as $s\hat{\tilde{m}} = TK\tilde{M}$. Let $\hat{K} = TK$, which represents the intrinsic parameters of camera corresponding to the projection $\hat{m}$. Once the internal parameter $\hat{K}$ is estimated in the coordinate system defined by T, the internal parameter k can be obtained by $K = T^{-1}\hat{K}$.

3.3 Nonlinear Optimization

The linear solution of the camera parameters is inaccurate, therefore a nonlinearly optimization of the parameters are required. As a classical nonlinear optimization algorithm, the LM algorithm combines the advantages of the steepest descent method and the Gauss-Newton method, and therefore can converge quickly. In 1D calibration, the optimization criterion is normally defined involving the projection of points in the calibration:

$$\sum_{i=1}^{N}(||a_i - a_i'(K, A_i)||^2 + ||b_i - b_i'(K, B_i)||^2 + ||c_i - c_i'(K, C_i)||^2) \tag{14}$$

where N is the number of captured pattern images. Firstly, as the camera parameters are solved by linear equation written in Eq. 13, the 3D coordinates of the marker points can be recovered according to Eq. 4. Secondly, the rotation angle which is denoted by (θ_i, ϕ_i) can be calculated, which is regarded as a constant that is used to update the 3D coordinates of B_i and C_i based on K and the 3D coordinates of A after each nonlinear optimization iteration. Thirdly, LM algorithm is used to optimize the K and the coordinates of point A in order to minimize the loss written in Eq. 14. In this way, the optimized camera parameters are obtained.

4 Improve Accurate 1D Calibration Algorithm Based on WSILA

4.1 Weighted Similarity-Invariant Linear Algorithm (WSILA)

According to the literature [16], the reciprocal of the standard deviation of the estimated relative depth from different images is used as the weight on the constraint equations in the similar invariant linear calibration algorithm, and a weighted similarity-invariant linear calibration algorithm with higher precision is proposed. According to Eq. 3, we have:

$$Lz_c\tilde{c} = (L - L_1)z_A\tilde{a} + L_1 z_B\tilde{b} \tag{15}$$

Equation 16 gives three linear equations of z_A, z_B and z_C and dividing both sides of the equal sign by z_A, the equation is equivalent to:

$$L(\tilde{c} - \tilde{b})\eta = (L - L_1)(\tilde{a} - \tilde{c}) \tag{16}$$

where

$$\eta = \frac{L_1(L - L_1)(\tilde{a} - \tilde{c})^T(\tilde{c} - \tilde{b})}{L_1^2||\tilde{c} - \tilde{b}||^2} \tag{17}$$

Therefore, the weight ρ of the constraint equation is:

$$\rho = \frac{1}{std(\eta)} \approx \frac{||\tilde{a} - \tilde{b}||}{\eta^2} \tag{18}$$

Equation 13 is equivalent to:

$$\rho \mathbf{V} x = \rho L^2 \mathbf{1} \tag{19}$$

The solution is then given by:

$$x = \rho L^2 (\rho \mathbf{V} (\rho \mathbf{V})^T)^{-1} (\rho \mathbf{V})^T \tag{20}$$

According to the obtained x, the symmetric matrix $\hat{\varpi}$ is represented. After a simple matrix operation, the parameter K can be finally obtained to realize the camera 1D calibration.

4.2 The Improved Nonlinear Optimization Procedure (INOP)

According to Zhang's 1D calibration algorithm, one can reconstruct the 3D coordinates of Bi after the linear step:

$$B_i = A_i + L \left[\sin\theta_i \cos\phi_i \quad \sin\theta_i \sin\phi_i \quad \cos\theta_i \right]^T \tag{21}$$

And then θ_i and ϕ_i can be calculated as written in Eq. 20:

$$\theta_i = arccos(\frac{z_{B_i} - z_{A_i}}{L}), \quad \phi_i = arccos(\frac{x_{B_i} - x_{A_i}}{L \sin\theta_i}) \tag{22}$$

In the previous algorithm, the 1D calibration object rotation angles θ_i and ϕ_i is considered as a constant during the nonlinear optimization procedure that is calculated according to Eq. 14. Instead, the constant θ_i and ϕ_i are used to update the B_i and C_i according to Eq. 21 that are used to calculated the loss according to Eq. 14. That is inaccurate since the z_{B_i}, z_{A_i}, x_{B_i}, x_{A_i} used in Eq. 22 are inaccurate. Consequently, the accuracy of the nonlinear optimization procedure is limited. To address this limitation, the work propose an improved nonlinear optimization procedure that update the 1D calibration object rotation angle θ_i and ϕ_i by the camera parameters and the coordinates of the rotation point coordinates should after each iteration, as is shown in Algorithm 1. And the objective function at this time is:

$$\sum_{i=1}^{N} \left(||a_i - a_i'(K, A_i, \theta_i, \phi_i)||^2 + ||b_i - b_i'(K, B_i, \theta_i, \phi_i)||^2 + ||c_i - c_i'(K, C_i, \theta_i, \phi_i)||^2 \right) \tag{23}$$

In the actual process, the 1D calibration object rotation angles θ_i and ϕ_i directly affect the 3D coordinates of the endpoints A and B_i, and the 3D coordinates are determined by the camera parameters and the image coordinates, wherein the image coordinates do not change, so when the camera parameters are updated, θ_i and ϕ_i also changes. Therefore, the improved nonlinear optimization procedure used in this paper: 1D calibration object rotation angle θ_i and ϕ_i should be updating by the camera parameters and the coordinates of the rotation point coordinates (show in Algorithm 1). And the objective function at this time is:

Algorithm 1. The improved nonlinear optimization procedure.

Input:

2D coordinates of the marker points $\tilde{m}_{mat}$, 1D calibration object lenth L ($L = ||B_i - A_i||$), λ ($\lambda = L_1/L$, $L_1 = ||C_i - A_i||$, A_i,B_i and C_i are the 3D coordinates of the marker points);

Output:

the camera parameter K

1: {Procedure. $lsqnonlin(\tilde{m}_{mat}, L, \lambda)$}
2: **while** flag is equal to 1 **do**
3: $[K, z_A, \eta] = WSILA(\tilde{m}_{mat}, L, \lambda)$, $\eta_i = -z_{B_i}/z_A$, z_{B_i} is the depth of the free endpoint B_i, z_A to the depth of the fixed endpoint A and η_i is the relative depth,which is the ratio of z_{B_i} to z_A;
4: $A_i = z_{A_i} K^{-1} \tilde{a_i}$, $\tilde{a_i}$ is the 2D image ponit of A_i;
5: $A_{mean} = mean(A_i)$; $z_A = A_{mean}(3)$; $z_{B_i} = -z_A * \eta_i$;
6: $B_i = z_{B_i} K^{-1} \tilde{b_i}$, $\tilde{b_i}$ is the 2D image point of B_i;
7: $\theta_i = arccos(\frac{z_{B_i} - z_A}{L})$, $\phi_i = arccos(\frac{x_{B_i} - x_A}{L * sin\theta_i})$, θ_i,ϕ_i are rotation angle of 1D calibration objects;
8: $\tilde{m}_{cal} = 3Dto2D(A, B)$, according to the standard pinhole imaging model, $\tilde{m}_{cal}$ is the updated 2D coordinates of the marker points;
9: Set the objective function F to $\sum_{i=1}^{N} \left(||a_i - a_i'(K, A_i, \theta_i, \phi_i)||^2 + ||b_i - b_i'(K, B_i, \theta_i, \phi_i)||^2 + ||c_i - c_i'(K, C_i, \theta_i, \phi_i)||^2\right)$;
10: Optimizing camera parameters K and the 3D coordinates of the fixed endpoint A using least squares, and update θ_i,ϕ_i;
11: **if** F reach the minimum value using the least squares **then**
12: $output$(K);
13: $flag = 0$;
14: **else**
15: $\tilde{m}_{mat} = \tilde{m}_{cal}$;
16: $flag = 1$;
17: **end if**
18: **end while**

5 Experimental Results

In this section, both simulation and laboratory experiments are conducted to test the performance of improved nonlinear optimization procedure. In detail, the 1D calibration accuracy of six algorithms are tested, including (a) Zhang's linear algorithm that is referred as ZLA; (b) Zhang's linear algorithm combined with the improved nonlinear optimization procedure that is referred as ZLA+INOP; (c) Franca et al.'s normalized linear algorithm that is referred as FNLA; (d) Franca et al.'s normalized linear algorithm combined with the improved nonlinear optimization procedure that referred as FNLA+INOP; (e) Weighted similarity-invariant linear algorithm that is referred as WSILA; (f) Weighted similarity-invariant linear algorithm combined with the improved nonlinear optimization procedure that is referred as WSILA+INOP.

5.1 Simulations

The pinhole camera model and the 1D camera calibration process are simulated in Matlab. The parameters of the simulated camera are set as follows: $\alpha = 1000$, $\beta = 1000$, $\gamma = 0$, $u_0 = 320$ and $v_0 = 240$. The image resolution is 640×80 pixels. A stick with a length of 70 cm is simulated, in which the 3D coordinates of the fixed point A is $[0 \quad 40 \quad 150]^T$, the other endpoint of the stick is B, while C is located in the middle of A and B. This experiment generates sticks with multiple random directions by sampling $\theta_i = [\pi/6, 5\pi/6]$, $\phi_i = [\pi/6, 5\pi/6]$ according to uniform distribution. The corresponding image coordinates a_i, b_i, c_i can be acquired through projecting A_i, B_i and C_i onto the image via pinhole camera model. Gaussian noise with a mean of 0 and different standard deviations (noise level) is added to the projected image points a, b and c, based on which the camera parameters are estimated using the six camera calibration algorithms separately. Then the relative errors of calibrated parameters are calculated, as

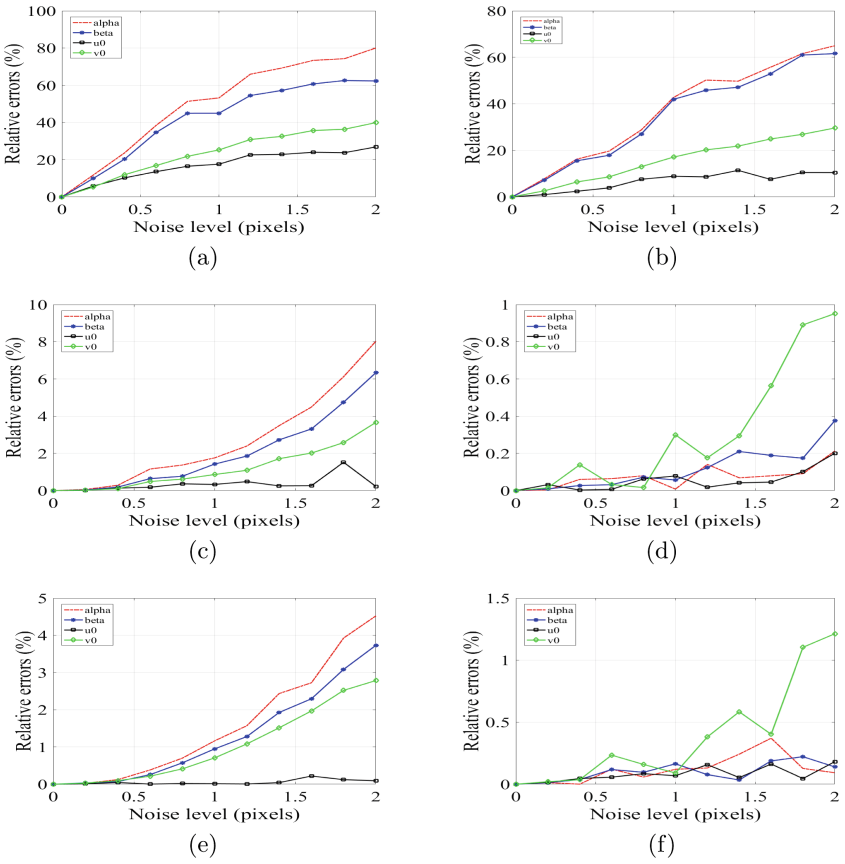

Fig. 2. Comparison of the relative errors of the six algorithms under the noise level from 0 to 2 pixels: (a) ZLA, (b) ZLA+INOP, (c) FNLA, (d) FNLA+INOP, (e) WSILA, and (f) WSILA+INOP.

shown in Fig. 2. In the experiment, the noise level was increased from 0 pixels to 2 pixels in a step of 0.2 pixels. For each noise level, 150 independent experiments were performed, and the average of each parameter was calculated.

As shown in Fig. 2, compared to ZLA (Fig. 2(a)), both FNLA (Fig. 2(c)) and WSILA (Fig. 2(e)) can greatly reduce the relative errors of calibrated parameters. Since it is taken into consideration of the different levels of importance of the constraint equations constructed from different poses, WSILA can provide better performance than FNLA. However, since the rotation angles θ_i and ϕ_i are not updated, the accuracy of WSILA is still limited, which is improved by the proposed nonlinear optimization procedure. When comparing the results of three combinations of (a) and (b), (c) and (d), (e) and (f), it is clear that the proposed nonlinear optimization procedure can greatly reduce the relative errors. For example, when the noise level is 2 pixels, the relative errors of camera parameters obtained by the combination of WSILA and the proposed nonlinear optimization procedure are smaller than 1.2%, while most of them are smaller than 0.2%. And the optimization process takes an average of 0.0078s to converge. Compared with the original WSILA, the average time calculated by WSILA+INOP algorithm increases from 1.0039s to 0.9941s. Therefore, the proposed nonlinear optimization procedure can greatly improve the camera calibration accuracy.

5.2 Laboratory Experiments

Fig. 3. Sample images of a 1D object used for camera calibration.

To verify the performance of proposed nonlinear optimization procedure, laboratory experiments are conducted. Three table tennis balls were fixed on a stick. The distance between adjacent balls are 133 cm (that is, L = 266 cm). One of the endpoints is fixed and the stick rotated 150 times around the fix endpoint, some of which are shown in Fig. 3. Then, the table tennis balls are detected through Hough circle detection algorithm, and the image coordinates of the marker points are measured accordingly. Then, the camera calibration is performed using the six algorithms. In order to evaluate the performance of the algorithms, the camera parameters are calibrated by Zhang's 2D camera calibration as a baseline, as is shown in Fig. 4. The experimental results are shown in Table 1.
From Table 1, the results of the WSILA combined with the nonlinear optimization algorithm (the proposed nonlinear optimization procedure) are closer to the Zhang's 2D calibration results compared to the other five methods. That is consistent with the simulation results.

Fig. 4. Sample image of the planar pattern used for camera calibration.

Table 1. 1D calibration results of cameras with different algorithms.

Solution	α	β	γ	u_0	v_0
ZLA	1230	1213	27.4	915	517
FNLA	1714	1717	22.5	1008	683
WSILA	1230	1213	27.4	915	517
ZLA+INOP	1339	1238	19.0	1002	544
FNLA+INOP	1750	1749	16.3	1004	689
WSILA+INOP	1747	1745	9.8	999	692
Zhang's 2D Camera Calibration	1742	1739	5.0	1005	754

6 Conclusion

Despite the flexibility of the Zhang's 1D calibration algorithm, the calibration results have large errors. To solve this problem, several solutions including simple data normalization and weighted similar invariant linear algorithms have been proposed to improve the calibration results. In this work, an improved nonlinear optimization procedure is proposed to further reduces the relative error of the camera parameters calibration results.

Through simulation experiments and laboratory experiments, the performance of the six 1D camera algorithms are studied. The results show that the method combining the weighted similarity invariant linear algorithm and the improved nonlinear optimization procedure has the best performance, which is better than the combination of the Zhang's linear algorithm and the improved nonlinear optimization procedure. It is also superior to the combination of the normalized and the improved nonlinear optimization procedure. According to the simulation results, when the noise level is 2 pixels, the relative errors of camera parameters obtained by the combination of WSILA and the improved nonlinear optimization procedure are smaller than 1.2%, while most of them are smaller than 0.2%. Through laboratory experiments, the parameters calibrated through the combination of WSILA and the improved nonlinear optimization procedure is the closest ones to the results from Zhang's 2D camera calibration. Therefore, the proposed nonlinear optimization procedure can greatly improve the camera calibration accuracy.

Acknowledgements. This work is financially supported in parts by the Fujian Provincial Department of Science and Technology of China (Grant No. 2019H0006 and 2018J01774), the National Natural Science Foundation of China (Grant No. 61601127), and the Foundation of Fujian Provincial Department of Industry and Information Technology of China (Grant No. 82318075).

References

1. Tsai, R., et al.: A versatile camera calibration technique for high-accuracy 3D machine vision metrology using off-the-shelf TV cameras and lenses. IEEE J. Rob. Autom. **3**(4), 323–344 (2003)
2. Yuan, T., Zhang, F., Tao, X.P.: Flexible geometrical calibration for fringe-reflection optical three-dimensional shape measurement. Appl. Opt. **54**(31), 9102–9107 (2015)
3. Yoo, J.S., et al.: Improved LiDAR-camera calibration using marker detection based on 3D plane extraction **13**(6), 2530–2544 (2018)
4. Duan, F., Wu, F., et al.: Pose determination and plane measurement using a trapezium. Pattern Recogn. Lett. **29**(3), 223–231 (2008)
5. Li, N., Hu, Z.Z., Zhao, B.: Flexible extrinsic calibration of a camera and a two-dimensional laser rangefinder with a folding pattern. Appl. Opt. **55**(9), 2270–2280 (2016)
6. Zhang, Z.Y.: Flexible camera calibration by viewing a plane from unknown orientation. In: IEEE International Conference on Computer Vision (1999)
7. Peng, E., Li, L.: Camera calibration using one-dimensional information and its applications in both controlled and uncontrolled environments. Pattern Recogn. **43**(1), 1188–1198 (2010)
8. Zhang, Z.Y.: Camera calibration with one-dimensional objects. IEEE Trans. Pattern Anal. Mach. Intell. **26**(7), 892–899 (2004)
9. Wang, L., Wang, W.W., et al.: A convex relaxation optimization algorithm for multi-camera calibration with 1D objects. Neurocomputing **215**, 82–89 (2016)
10. Lv, Y.W., Liu, W., et al.: Methods based on 1D homography for camera calibration with 1D objects. Appl. Opt. **57**(9), 2155–2164 (2018)
11. Akkad, N.E., Merras, M., et al.: Camera self-calibration with varying intrinsic parameters by an unknown three-dimensional scene. Int. J. Comput. Graphics. **30**(5), 519–530 (2014)
12. Sun, Q., Wang, X., et al.: Camera self-calibration with lens distortion. Optik Int. J. Light Electron Optics. **127**(10), 4506–4513 (2016)
13. Finsterle, S., Kowalsky, M.B.: A truncated Levenberg-Marquardt algorithm for the calibration of highly parameterized nonlinear models **37**(5), 731–738 (2011)
14. Li, J.H., Zheng, W.X., et al.: The Parameter estimation algorithms for Hammerstein output error systems using Levenberg-Marquardt optimization method with varying interval measurements. IFAC Papersonline **48**(8), 457–462 (2015)
15. Franca, J.D., Stemmer, M.R., et al.: Revisiting Zhang's 1D calibration algorithm. Pattern Recogn. **43**(3), 1180–1187 (2010)
16. Kunfeng, S., Qiulei, D., Fuchao, W.: Weighted similarity-invariant linear algorithm for camera calibration with rotating 1D objects. IEEE Trans. Image Process. **21**(8), 3806–3812 (2012)
17. Wang, L., Duan, F.: Zhang's one-dimensional calibration revisited with the heteroscedastic error-in-variables model. In: 8th IEEE International Conference on Image Processing. IEEE (2011)